MAGNETOTAIL SUBSTORM FEATURES FROM MULTI-POINT OBSERVATIONS

A.T.Y. Lui[(1)], Y. Zheng[(1)], A. Balogh[(2)], P. W. Daly[(3)], M. W. Dunlop[(4)], T. A. Fritz[(5)], G. Gustafsson[(6)], S. Livi[(1)], S. B. Mende[(7)], C. J. Owen[(8)], R. F. Pfaff[(9)], H. Rème[(10)], Y. Zhang[(1)], and Q. Zong[(5)]

[(1)]JHU/APL, 11100 Johns Hopkins Rd., Laurel, MD 20723-6099, USA
[(2)]Imperial College, Department of Space and Atmospheric Physics, London, UK
[(3)]Max-Planck-Institut für Aeronomie, D-37191 Katlenburg-Lindau, Germany
[(4)]Space Science and Technology Department, RAL, Chilton, Didcot, Oxfordshire OX11 0QX, UK
[(5)]Center for Space Physics, Boston University, 725 Commonwealth Ave., Boston, MA 02215, USA
[(6)]Swedish Institute of Space Physics, Uppsala Division, S-755 91 Uppsala, Sweden
[(7)]University of California, Space Sciences Laboratory, 7 Gauss Way, Berkeley, CA 94720-7450, USA
[(8)]Mullard Space Science Laboratory, University College London, Holmbury St. Mary, Dorking, Surrey, RH5 6NT, UK
[(9)]Laboratory for Solar and Space Physics, NASA Goddard Space Flight Center, Greenbelt, MD 20771, USA
[(10)]CESR, BP4346, 31028 Toulouse Cedex 4, Toulouse, France

ABSTRACT

We examine several dipolarizations and a reversal of plasma flow detected by Cluster at the downstream distance of ~19 R_E in the midnight sector of the magnetotail on August 22, 2001. These substorm features occurred during a sequence of substorm activity seen by the IMAGE/FUV imager. Findings consistent with previous reports are the following: (1) there is generally a decrease of the *z*-component of the magnetic field (B_z) prior to dipolarization; (2) the onset of dipolarization can precede the onset of significant plasma flow; (3) dipolarization is quite episodic in nature, consisting of multiple increases and decreases of the B_z component. New features revealed in this study are the following: (1) the turbulent region associated with dipolarization can exhibit dynamo effect as well as dissipation, (2) the *x*-component of the Lorentz force $(j\times B)_x$ does not change sign at plasma flow reversal although the other two components do (indicative of changes in the magnetic stress consistent with shifting dominance of multiple activity sites rather than a tailward movement of a single activity site as commonly assumed), and (3) the frozen-in condition breaks down during dipolarization in several regions where the B_z component and the total magnetic field strength have large values, different from the expectation of the diffusion region associated with magnetic reconnection.

1. INTRODUCTION

Plasma environment in the Earth's magnetotail has been studied since the early days of the Vela satellites in the late 1960's (see, e.g., [1]). Plasma flows were inferred from these early measurements even though the plasma detectors and the satellite spin axis orientation were not ideally designed to obtain accurate determination of plasma flow direction. It has been recognized in early substorm research that high-speed plasma flows occur during geomagnetic active periods. The lack of multi-point observations in the magnetotail and the ambiguity in differentiating temporal from spatial variations have posed major obstacles in advancing our understanding of substorm phenomena in the magnetotail. In spite of these deficiencies, attempts have been made to construct global substorm development in the magnetotail from single-point observations through statistical studies [2-5]. Synoptic maps of substorm features from these studies have enabled substorm models incorporating disturbances in the magnetotail [6-7].

The ISEE-1/2 mission demonstrated the power of multi-point measurements from satellites flying in close formation. Subsequently, the International Solar Terrestrial Physics (ISTP) program has brought the prowess of multi-point magnetospheric observations to the forefront of space research. The Cluster-II mission elevates the capability of ISEE-1/2 and ISTP missions even further by the ability to determine gradients in three-dimensions as well as differentiate temporal from spatial variations. This capability provides valuable constraints in data interpretation on magnetotail dynamics.

It is evident that the new capability of Cluster can help to advance our understanding of substorm phenomena. Several investigations have utilized Cluster to examine substorm phenomena in the tail [8-12]. In this paper, we explore some substorm features observed by Cluster on 2001 August 22 in some details. This event study is selected based on the availability of global auroral images from IMAGE simultaneous with Cluster observations so that substorm onset and subsequent intensifications can be identified and related to magnetotail disturbances. The main focus of this study are (1) the comparison between dipolarization and plasma flow onsets including an examination of the

Proceedings Cluster and Double Star Symposium – 5th Anniversary of Cluster in Space, Noordwijk, The Netherlands, 19 - 23 September 2005 (ESA SP-598, January 2006)

related magnetic stress, and (2) the magnetic stress in a plasma flow reversal interval when tailward plasma flow accompanied by southward magnetic field changed to earthward plasma flow accompanied by northward magnetic field. These topics may be used to validate or falsify existing substorm models. In particular, the traditional interpretation of this type of plasma flow reversal is the tailward movement of an X-type neutral line, a key element of the near-Earth neutral line model for substorms. We shall show that there are features in this flow reversal interval that do not fit well with this traditional interpretation. A more plausible interpretation of the flow reversal event discussed here is the shifting role of different activity sites in dominating the plasma behavior at a given point of observation.

2. OBSERVATIONS

The ground-station magnetic activity on 2001 August 22 is provided by the AU/AL indices shown in Fig. 1. For the time interval of interest, 0900-1200 UT, the AL index showed the strengthening of auroral electrojet signifying substorm development. The more definitive signature of substorm onset was registered by the IMAGE/FUV imager at ~0920 UT, with a sizeable auroral bulge seen at ~0926 UT, as shown in Fig. 2. Multiple substorm intensifications followed as indicated by the series of auroral images. During this period, Cluster was near its apogee in the magnetotail and crossed the neutral sheet from north to south, as shown in Fig. 3 with measurements from C3. Shown in the panels are the number density, the ion temperature (red trace), the x- and y-components of plasma flow, the y-components of electric field and $-V\times B$ (cross-product of plasma flow and magnetic field - red trace), the x- and y-components of the magnetic field, and the z-component of the magnetic field. The plasma measurements were taken by CIS/HIA [13], which are used in this entire study. The electric and magnetic field measurements were obtained by EFW [14] and FGM [15], respectively. The measurements show several dipolarizations of the magnetic field and plasma flow reversals, which will be discussed in detail later. It also can be noted that the y-components of electric field and $-V\times B$ matched well in general but significant deviations can also be seen intermittently.

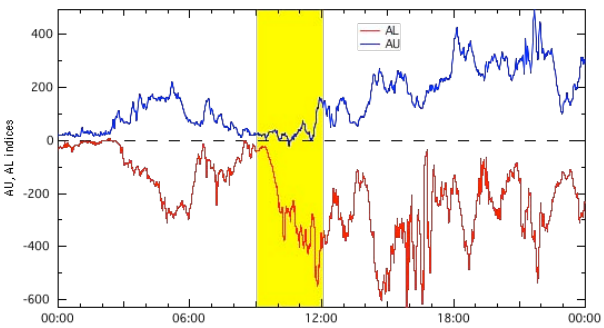

Fig.1. AU and AL indices for 2001 August 22.

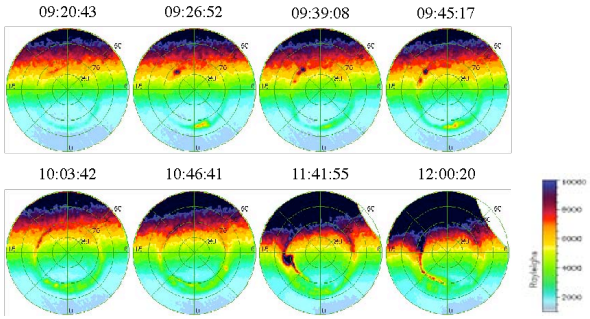

Fig. 2. Global auroral images from IMAGE/FUV.

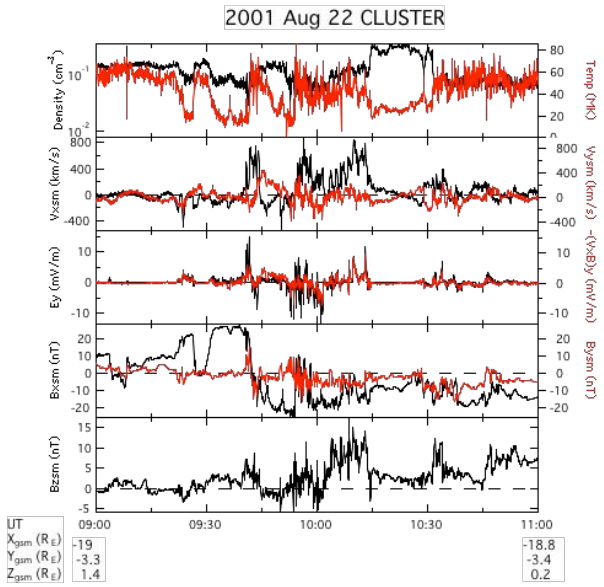

Fig. 3. Overview of magnetotail activity at Cluster.

The dimension of the tetrahedron formed by the four Cluster satellites was ~2000 km, with C3 at its apex south of the tetrahedron base, see Fig. 4. Cluster data for this period have been studied previously with focus on MHD oscillation modes of the plasma sheet rather than substorm features as aimed here [16-18].

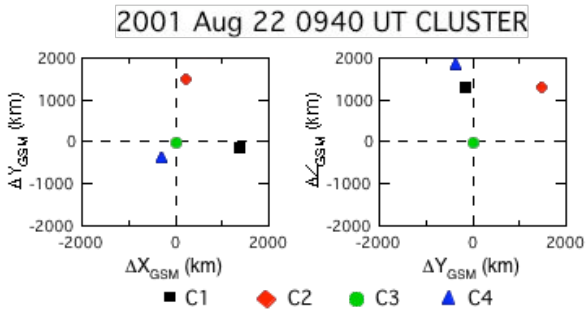

Fig. 4. Relative locations of Cluster spacecraft.

2.1 Dipolarization and Plasma Flow

The first set of two dipolarizations is shown in Fig. 5, where measurements from different satellites are given in different colors. Plasma flows shown are components perpendicular to the magnetic field. The geocentric solar

magnetospheric (GSM) coordinates are used throughout this study. Cluster satellites were located at ~(-18.9, -3.3, 1.1) R_E and detected dipolarization at ~0939 and ~0940 UT, which were ~20 min after the substorm onset seen by IMAGE/FUV data. Based on the T96 magnetic field model [19], the location of Cluster projected along the magnetic field line to the ionosphere at this time is 67.5° MLat and 1.1 MLT, just poleward of the auroral bulge seen by IMAGE/FUV at ~0926 UT. Prior to dipolarization, southward dipping of the magnetic field (i.e., southward B_z component small compared with the total magnetic field strength) was seen by all four satellites, suggesting plasma sheet thinning before dipolarization onset. Note that dipolarization preceded the occurrence of fast plasma flow. Highly structured electric and magnetic fields, indicative of a turbulent region, were detected after dipolarization. The E_y component exhibited a kink mode behavior, i.e., duskward in the northern part of the tail and dawnward in the southern part of the tail. Only the E_y component is examined in this study because it is the most reliable component from EFW.

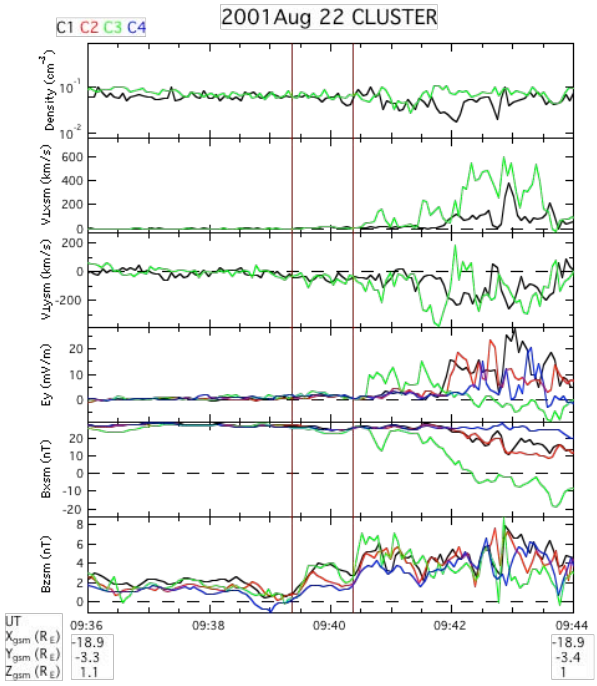

Fig. 5. Dipolarizations at ~0939 and ~0940 UT.

Another set of two dipolarizations at ~1002 and ~1004 UT is shown in Fig. 6. The E_y component was strong prior to dipolarization, maintaining opposite signs in the two halves of the magnetotail as noted in the previous interval in Fig. 5. There was fast earthward plasma flow ~1 min before the first dipolarization when the B_z component was southward. However, at the dipolarization onset times, there was no evidence of fast plasma flows. The dipolarization onsets appeared to be simultaneous at all four satellites with the spin-averaged data. After dipolarization, the E_y component diminished its strength.

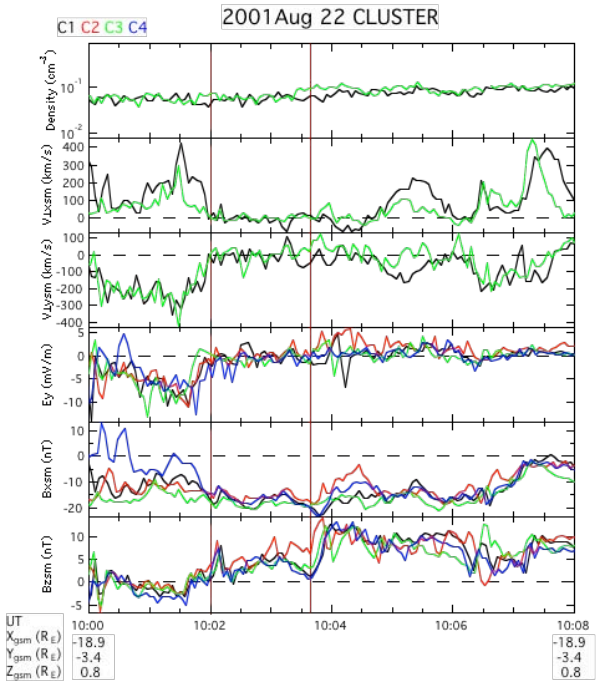

Fig. 6. Dipolarizations at ~1002 and ~1004 UT.

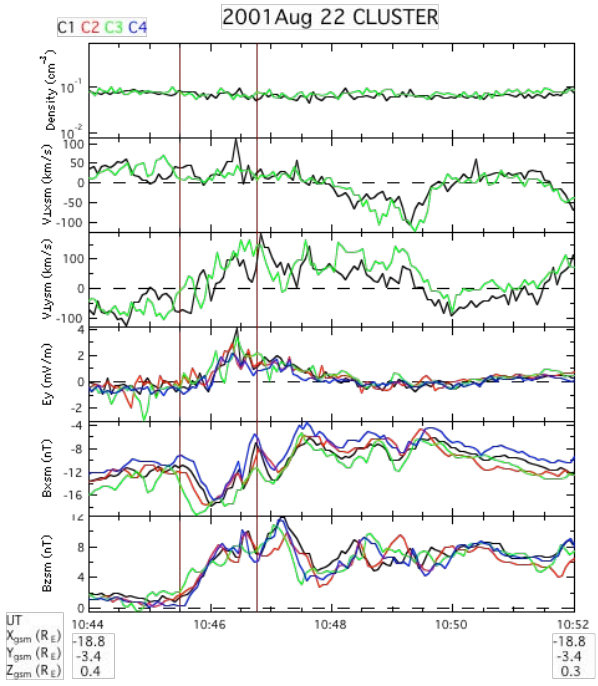

Fig. 7. Dipolarizations at ~1044 and ~1052 UT.

The final set of two dipolarizations during this interval occurred at ~1045 and ~1047 UT, as shown in Fig. 7. Around the dipolarization onset times, plasma flow was relatively slow. The V_x component was below 50 km/s while V_y was less than 200 km/s. These flow speeds are well below the level qualified for bursty bulk flow, which is often taken to be 300-400 km/s.

In general, it is difficult to use timing analysis to determine the propagation of the dipolarization front since the detailed B_z profile at each satellite was different from the others. These characteristics suggest that the magnetic field profile changed significantly as dipolarization proceeded from one satellite to the next and/or the front was highly non-uniform spatially. However, for some dipolarizations, the temporal sequence seems to be clear. For instance, for the ~1004 UT onset, the sequence was C1-C2-C3-C4, indicating that dipolarization propagated from the earthward-duskward direction. For the ~1045 UT onset, the sequence was C2-C1-C3-C4, indicating that dipolarization propagated from the duskward-earthward direction. The observed dipolarization propagation direction is consistent with previous report of tailward propagation of dipolarization [4].

2.2 Energetics Associated With Dipolarization

The curlometer technique [20-22] is used to determine the current density and plasma parameters associated with current density in these dipolarizations. Fig. 8 shows the result for the dipolarizations at ~0939 and ~0940 UT. The panels from top to bottom show, respectively, the three components of current density, the three components of the Lorentz force ($j\times B$), the dissipation/dynamo term $j_y\langle E_y\rangle$ (the angle brackets indicate averaging over the four spacecraft), and the B_z component from all four spacecraft as a reference. Prior to dipolarization, the current density was low. This is to be expected since the satellites were not near the neutral sheet region as indicated by the strength of the B_x component. After dipolarization, the satellites became embedded within the central plasma sheet and observed higher current density than before. The $(j\times B)_z$ component was most significant and pointed towards the neutral sheet. This implies a strong plasma pressure gradient with the high pressure towards the neutral sheet, which is the expected pressure gradient direction. The $(j\times B)_x$ component was pointing earthward, consistent with the expected enhancement in the earthward-directed magnetic stress during dipolarization [23]. The dissipation/dynamo term was mainly positive, but it became negative momentarily in the turbulent region after the dipolarization onset.

Fig. 9 shows the same current parameters for the second set of dipolarizations. At the beginning of the interval, the satellites were within the central plasma sheet (the B_x component was small). The cross-tail current component j_y was relatively strong. After dipolarization, j_y became weaker, the three components of $j\times B$ varied significantly, and the $j_y\langle E_y\rangle$ term changed sign frequently in the turbulent magnetic field region. Similar behavior of these plasma parameters was seen for the third set of dipolarizations as well.

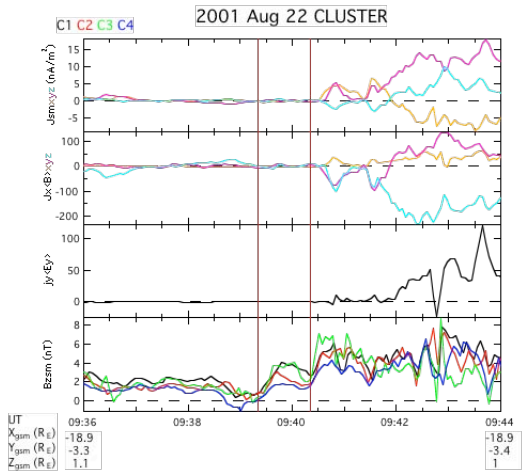

Fig. 8. Current parameters for ~0939 and ~0940 UT dipolarizations.

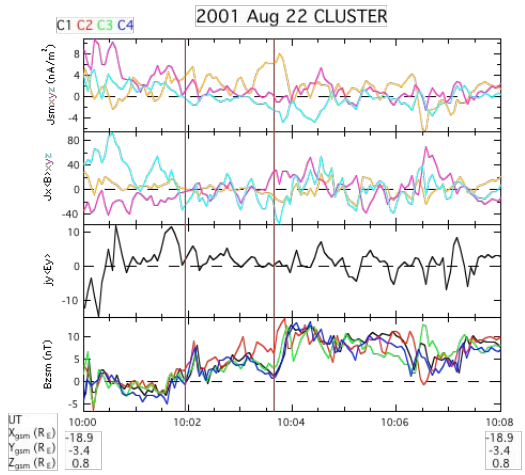

Fig. 9. Current parameters for ~1002 and ~1004 UT dipolarizations.

2.3 Plasma Flow Reversal

There was a plasma flow reversal during this interval of activity, as shown in Fig. 10. The panels show the number density and V_x component from CIS/HIA on C1 and C3, E_y and three components of magnetic field from all four spacecraft. The plasma flow reversal at ~0954 UT was accompanied by a reversal in the B_z component. There was a reduction in number density at plasma flow reversal. Note that both C1 and C3 crossed the neutral sheet just around the flow reversal time and yet the number density at the neutral sheet was lower there than earlier in the interval when the spacecraft was further away from the neutral sheet. Thus, there was a substantial loss of plasma in the neutral sheet at that time.

The current parameters during the flow reversal interval are shown in Fig. 11. The j_y component stayed positive while the j_x component reversed sign from positive to negative at plasma flow reversal. An interesting feature is the sign reversal of the y- and z-components of $j\times B$ at

flow reversal while the x-component did not show any reversal. This indicates that the magnetic stress in the y- and z-directions changed at flow reversal but not in the x-direction. The $j_y<E_y>$ term is quite variable, indicating the occasional presence of the dynamo effect in addition to dissipation.

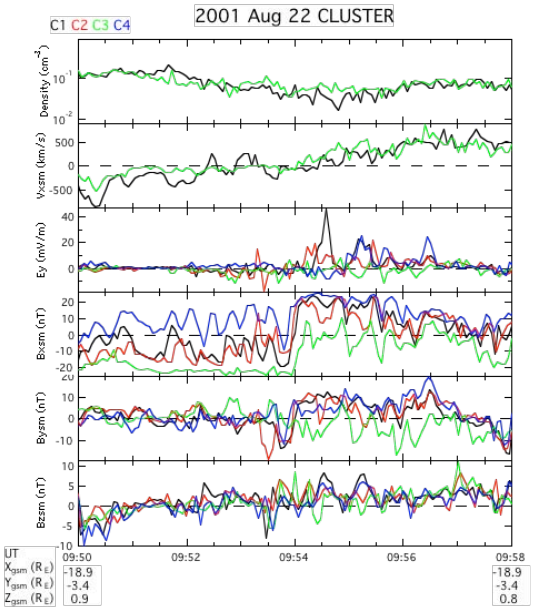

Fig. 10. A plasma flow reversal detected by Cluster.

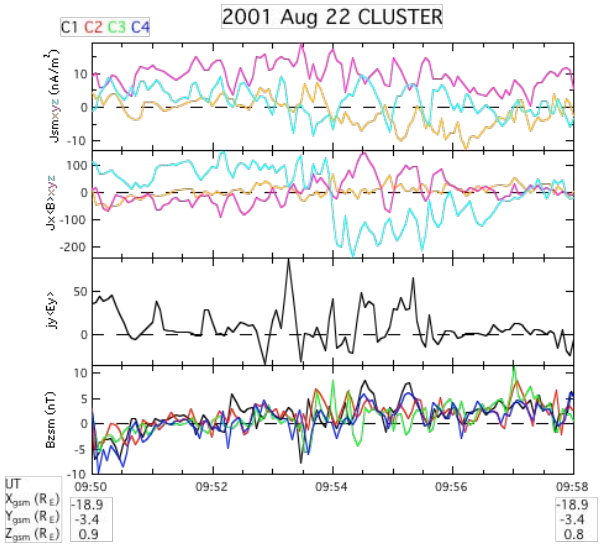

Fig. 11. Plasma parameters associated with current density during a plasma flow reversal.

2.4 Breakdown in Frozen-in Condition

During this sequence of substorm activity, there were several brief instances in which the frozen-in condition was violated, i.e. $E \neq -V\times B$. Fig. 12 shows three intervals for which the y-components of E and $-V\times B$ are compared together with the three components of the local magnetic field. The first interval encompasses the dipolarization and the data were taken by C3. The second interval is during the turbulence encountered after dipolarization and the third is the flow reversal period, both showing data from C1. For the first interval, the two quantities matched well prior to dipolarization. However, significant differences occurred afterwards. In the turbulent region (second interval), the two quantities did not agree in general. For the third interval, large discrepancies existed intermittently. Note that the breakdown of frozen-in condition occurred when the magnitudes of B and B_z had large values, indicating that these regions are not within the diffusion region around an X-line where the magnetic field is expected to be weak.

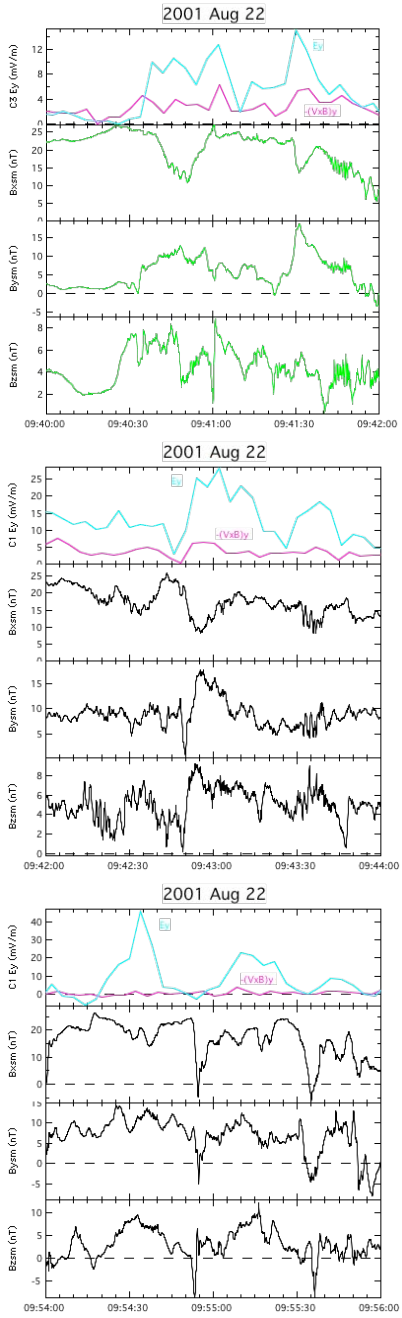

Fig. 12. Three intervals when the frozen-in condition breaks down.

The various terms of the generalized Ohm's law were examined to determine the cause for the violation of the frozen-in condition, i.e., the non-MHD behavior. It is found that the Hall term was the most significant non-negligible term, followed by the electron pressure gradient term. The electron inertial term was negligible. However, the magnitude of the anomalous resistivity term is unclear due to the lack of information on the value of anomalous resistivity. For example, it is found that at 0954:35 UT, in SI units, $(E+V\times B)_y \sim 4.6\times10^{-2}$, $(j\times B)_y/Nq \sim 3.8\times10^{-2}$, $-(\nabla\bullet\mathbf{P}_e)_y/Nq \sim 5.9\times10^{-4}$, and $(m_e/q^2)\ d(j_y/N)/dt \sim -1.6\times10^{-7}$, where the new symbols are the number density N, the unit electric charge q, the electron pressure tensor $\mathbf{P}_e$, and the electron mass m_e.

3. SUMMARY AND DISCUSSION

The magnetotail behavior during a sequence of substorm activity on 2001 August 22 is examined with data from Cluster satellites that were at ~19 R_E downstream in the midnight sector. Several magnetic field dipolarizations were detected. Dipolarization was episodic, consisting of multiple increases and decreases of the B_z component. Each dipolarization front was followed by an interval of highly variable electric and magnetic fields as well as variable j_yE_y sign, suggesting the occurrence of turbulence in the dipolarization process and also the presence of dynamo effect as well as dissipation in the turbulent region. In general, no fast (>300 km/s) plasma flow occurred before dipolarization during this interval. This is evidence for a non-MHD feature, suggesting dipolarization to be related to a kinetic process. A decrease of B_z prior to dipolarization was also generally seen, suggesting plasma sheet thinning prior to dipolarization. During a plasma flow reversal, there were sign changes in the magnetic stress in the y- and z-directions but not in the x-direction. This feature suggests that the plasma flow reversal arose from shifting dominance of multiple activity sites rather than movement of a single activity site. Note that tailward movement of a near-Earth neutral line should give rise to a changing sign (from negative to positive) of magnetic stress in the x-direction, which is not seen here. It is unclear how general this result is for flow reversal events. At the very least, however, this finding demonstrates that plasma flow reversal from tailward to earthward is not necessarily due to tailward retreat of a single magnetic reconnection site.

Some of these results summarized above are not new. A decrease of B_z prior to dipolarization has been reported previously by several researchers [24-28]. Different interpretations were considered, such as plasma sheet thinning from rarefaction wave passage [24], current intensification prior to dipolarization [25, 26], eastward expansion of substorm current wedge [27], and flux rope associated with earthward plasma flow [28]. In the events shown here, decrease of the z-component of the magnetic field prior to dipolarization was not associated with plasma flow, thus ruling out the flux rope interpretation. For the interpretation of eastward expansion of the substorm current wedge, it predicts that the B_y peak will coincide with the zero crossing of the B_z component. In these events, the associated B_y component did not show such a trend and thus ruling out this interpretation also. The interpretations of plasma sheet thinning from rarefaction wave passage and current intensification are essentially the same since the former emphasizes the boundary while the latter emphasizes the current density enhancement as a result of plasma sheet thinning. The observed field characteristics (such as southward dipping of the magnetic field) are consistent with these interpretations.

Another quite well known aspect of dipolarization is its episodic behavior [25, 27]. Dipolarizations can occur in succession within 2 min., e.g., events reported in [27]. The lack of plasma flow at the time of dipolarization has also been found previously [29, 27].

The new features reported here are (1) the variability in the dynamo/dissipation effect within the turbulent region following the dipolarization, (2) the absence of the sign reversal in the x-component of the Lorentz force in association with plasma flow reversal - other components reversing in sign instead, and (3) the breakdown of the frozen-in condition in several regions associated with the dipolarization activity. These regions do not exhibit low magnetic field strength expected for the diffusion region around a magnetic reconnection site. Furthermore, these regions had large B_z component, suggesting that they are not associated with the separatrix layer of magnetic reconnection, which should coincide with the plasma sheet boundary, where the B_z component would be small. The violation of the frozen-in condition may be due to a kinetic plasma process, such as the kinetic ballooning instability [30, 31], the current-driven electromagnetic ion cyclotron instability [32], the cross-field current instability [33], or the entropy antidiffusion instability [34], that are related to current disruption and dipolarization. Large amplitude high frequency waves expected from the excitation of the cross-field current instability have been observed by Geotail in high-time resolution wave data during dipolarization without accompanying plasma flow [27]. This aspect will be considered in future extension of this work.

Many articles in the literature on magnetotail dynamics interpreted observations in terms of magnetic reconnection only without considering alternative explanations. However, many of the observed features are basically products of ions decoupling from electrons in the plasma, a natural outcome of a kinetic plasma process. Therefore, the observed features are not unique to magnetic reconnection alone. For example, the generation of the so-called Hall current system (together with the quadruple out-of-the-plane magnetic

perturbations) associated with magnetic reconnection [35] is essentially (and more appropriately called) a meridional current system when ions become unmagnetized while electrons are not. It is pointed out [36, 37] that such a current system can be generated by the onset of a kinetic plasma process like the cross-field current instability. A bipolar electric field signature, as seen in some dynamic magnetotail events [11], can also be created as a result. It is prudent for future investigations of magnetotail dynamics to distinguish these models by identifying observational features that are not common among these different models.

4. ACKNOWLEDGMENT

This work was supported in part by NSF Grant ATM-00135667, NASA Grant NNG04G128G, and NASA Contract NAS5-02099 to The Johns Hopkins University Applied Physics Laboratory.

5. REFERENCES

1. Hones, E. W., Jr., Plasma flow in the plasma sheet and its relation to substorms, *Radio Sci., 8*, 979, 1973.

2. Lui, A. T. Y., E. W. Hones, Jr., F. Yasuhara, S.-I. Akasofu, and S. J. Bame, Magnetotail plasma flow during plasma sheet expansions: Vela 5 and 6 and IMP 6 observations, *J. Geophys. Res., 82*, 1235, 1977.

3. Lui, A. T. Y., K. Liou, P. T. Newell, C.-I. Meng, S.-I. Ohtani, S. Kokubun, T. Ogino, M. Brittnacher, and G. Parks, Plasma and magnetic flux transport associated with auroral breakups, *Geophys. Res. Lett.*, *25*, 4059-4062, 1998.

4. Jacquey, C., J. A. Sauvaud, J. Dandouras, and A. Korth, Tailward propagating cross-tail current disruption and dynamics of near-Earth tail: A multi-point measurement analysis, *Geophys. Res. Lett., 20*, 983-986, 1993.

5. Miyashita, Y., S. Machida, K. Liou, T. Mukai, Y. Saito, H. Hayakawa, C.-I. Meng, G. K. Parks, Evolution of the magnetotail associated with substorm auroral breakups, *J. Geophys. Res.*, *108*, A9, 10.1029/2003JA009939, 2003.

6. Hones, E. W., Jr., and K. Schindler, Magnetotail plasma flow during substorms: a survey with IMP 6 and IMP 8, *J. Geophys. Res., 84*, 7155, 1979.

7. Lui, A. T. Y., A synthesis of magnetospheric substorm models, *J. Geophys. Res.*, *96*, 1849-1856, 1991.

8. Nakamura, R., W. Baumjohann, R. Scho¨del, M. Brittnacher, V. A. Sergeev, M. Kubyshkina, T. Mukai, and K. Liou, Earthward flow bursts, auroral streamers, and small expansions, *J. Geophys. Res.*, *106*, 10,791, 2001.

9. Nakamura, R., W. Baumjohann, B. Klecker, Y. Bogdanova, A. Balogh, H. Re`me, J. M. Bosqued, I. Dandouras, J. A. Sauvaud, K.-H. Glassmeier, L. Kistler, C. Mouikis, T. L. Zhang, H. Eichelberger, and A. Runov, Motion of the dipolarization front during a flow burst event observed by Cluster, *Geophys. Res. Lett.*, *29*(20), 1942, doi:10.1029/2002GL015763, 2002.

10. Nakamura, R., W. Baumjohann, A. Runov, M. Volwerk, T. L. Zhang, B. Klecker, Y. Bogdanova, A. Roux, A. Balogh, H. Rème, J. A. Sauvaud, and H. U. Frey, Fast flow during current sheet thinning, *Geophys. Res. Lett.*, *29*(23), 2140, doi:10.1029/2002GL016200, 2002.

11. Nakamura, R., W. Baumjohann, T. Nagai, M. Fujimoto, T. Mukai, B. Klecker, R. Treumann, A. Balogh, H. Rème, J. A. Sauvaud, L. Kistler, C. Mouikis, C. J. Owen, A. N. Fazakerley, J. P. Dewhurst, and Y. Bogdanova, Flow shear near the boundary of the plasma sheet observed by Cluster and Geotail, *J. Geophys. Res.*, *109*, A05204, doi:10.1029/2003JA010174, 2004.

12. Runov, A., R. Nakamura, W. Baumjohann, R. A. Treumann, T. L. Zhang, M. Volwerk, Z. Vörös, A. Balogh, K.-H. Glaßmeier, B. Klecker, H. Rème, L. Kistler, Current sheet structure near magnetic X-line observed by Cluster, *Geophys. Res. Lett. 30* (11), 10.1029/2002GL016730, 2003.

13. Rème, H., et al., First multispacecraft ion measurements in and near the Earth's magnetosphere with the identical Cluster ion spectrometry (CIS) experiment, *Ann. Geophys.*, *19*, 1303-1354, 2001.

14. Gustafsson, G., R. Boström, B. Holback, G. Holmgren, A. Lundgren, K. Stasiewicz, L. Åhlén, F. S. Mozer, D. Pankow, P. Harvey, P. Berg, R. Ulrich, A. Pedersen,, R. Schmidt, A. Butler, A. W. Fransen, D. Klinge, M. Thomsen, C.-G. Fälthammar, P.-A. Lindqvist, S. Christenson, J. Holtet, B. Lybekk, T. A. Sten, P. Tanskanen, K. Lappalainen, and J. Wygant, The electric field and wave experiment for the Cluster mission, *Space Sci. Rev.*, *79*, 137-156, 1997.

15. Balogh, A., C. M. Carr, M. H. Acuna, M. W. Dunlop, T. J. Beek, P. Brown, K.-H. Fornacon, E. Georgescu, K.-H. Glassmeier, J. Harris, G. M. Musmann, T. Oddy, and K. Schwingenschuh, The Cluster magnetic field investigation: overview of in-flight performance and initial results, *Ann. Geophys.*, *19*, 1207–1217, 2001.

16. Louarn, P., G. Fruit, E. Budnik, J. A. Sauvaud, C. Jacquey, D. Le Quéau, H. Rème, E. Lucek, and A.

Balogh, On the propagation of low-frequency fluctuations in the plasma sheet: 1. Cluster observations and magnetohydrodynamic analysis, *J. Geophys. Res.*, *109*, A03216, doi:10.1029/2003JA010228, 2004.

17. Fruit, G., P. Louarn, E. Budnik, J. A. Sauvaud, C. Jacquey, D. Le Quéau, H. Rème, E. Lucek, A. Balogh, and N. Cornilleau-Wehrlin, On the propagation of low-frequency fluctuations in the plasma sheet: 2. Characterization of the MHD eigenmodes and physical implications, *J. Geophys. Res.*, *1 0 9*, A03217, doi:10.1029/2003JA010229, 2004.

18. Volwerk, M., K.-H. Glassmeier, A. Runov, W. Baumjohann, R. Nakamura, T. L. Zhang, B. Klecker, A. Balogh, and H. Rème, Kink mode oscillation of the current sheet, *Geophys. Res. Lett.*, *30*(6), 1320, doi:10.1029/2002GL016467, 2003.

19. Tsyganenko, N. A., Modeling the Earth's magnetospheric magnetic field confined within a realistic magnetopause, *J. Geophys. Res.*, *100*, 5599-5612, 1995.

20. Chanteur, G., Spatial interpolation for four spacecraft: Theory, in *Analysis Methods for Multi-Spacecraft Data*, *ISSI Sci. Rep. SR-001*, ed. by G. Paschmann and P. Daly, pp. 349–369, Eur. Space Agency, Paris, 1998.

21. Chanteur, G. and C. C. Harvey, Spatial interpolation for four spacecraft: Application to magnetic gradients, *Analysis Methods for Multi-Spacecraft Data*, *ISSI Sci. Rep. SR-001*, ed. G. Paschmann and P. W. Daly, 371-393, 1998.

22. Robert, P., A. Roux, C. C. Harvey, M. W. Dunlop, P. W. Daly, K.-H. Glassmeier, Tetrahedron Geometric factors, in *Analysis Methods for Multi-Spacecraft Data*, *ISSI Sci. Rep. SR-001*, ed. by G. Paschmann and P. Daly, pp. 323–348, Eur. Space Agency, Paris, 1998.

23. Lui, A. T. Y., P. H. Yoon, and C.-L. Chang, Quasi-linear analysis of ion Weibel instability, *J. Geophys. Res.*, *98*, 153-163, 1993.

24. Lui, A. T. Y., C.-I. Meng, and S.-I. Akasofu, Search for the magnetic neutral line in the near-earth plasma sheet, l. Critical re-examination of earlier studies of magnetic field observations, *J. Geophys. Res.*, *81*, 5934-5940, 1976.

25. Lui, A. T. Y., R. E. Lopez, S. M. Krimigis, R. W. McEntire, L. J. Zanetti, and T. A. Potemra, A case study of magnetotail current sheet disruption and diversion, *Geophys. Res. Lett.*, *15*, 721, 1988.

26. Ohtani, S., K. Takahashi, C. T. Russell, Radial expansion of the tail current disruption during substorms: A new approach to substorm onset region, *J. Geophys. Res., 97*, 3129-3136, 1992.

27. Shiokawa, K., Y. Miyashita, I. Shinohara, and A. Matsuoka, Decrease in B_z prior to the dipolarization in the near-Earth plasma sheet, *J. Geophys. Res.*, *110*, A09219, doi:10.1029/2005JA011144, 2005.

28. Slavin, J. A., R. P. Lepping, J. Gjerloev, D. H. Fairfield, M. Hesse, C. J. Owen, M. B. Moldwin, T. Nagai, A. Ieda, and T. Mukai, Geotail observations of magnetic flux ropes in the plasma sheet, *J. Geophys. Res.*, *108*(A1), 1015, doi:10.1029/2002JA009557, 2003.

29. Lui, A. T. Y., K. Liou, M. Nosé, S. Ohtani, D. J. Williams, T. Mukai, K. Tsuruda, S. Kokubun, Near-Earth dipolarization: Evidence for a non-MHD process, *Geophys. Res. Lett.*, *26*, 2905, 1999.

30. Cheng, C. Z. and A. T. Y. Lui, Kinetic ballooning instability for substorm onset and current disruption observed by AMPTE/CCE, *Geophys. Res. Lett.*, *25*, 4091-4094, 1998.

31. Roux, A., S. Perraut, P. Robert, A. Morane, A. Pedersen, A. Korth, G. Kremser, B. Aparicio, D. Rodgers, R. Pellinen, Plasma sheet instability related to the westward traveling surge, *J. Geophys. Res.*, *96*, 17697-17714, 1991.

32. Perraut, S., O. Le Contel, A. Roux, and A. Pedersen, Current-driven electromagnetic ion cyclotron instability at substorm onset, *J. Geophys. Res.*, *105*, 21097-21107, 2000.

33. Lui, A. T. Y., C.-L. Chang, A. Mankofsky, H.-K. Wong, and D. Winske, A cross-field current instability for substorm expansions, *J. Geophys. Res.*, *96*, 11389-11401, 1991.

34. Lee, L. C., L. Zhang, A. Otto, G. S. Choe, and H. J. Cai, Entropy antidiffusion instability and formation of a thin current sheet during geomagnetic substorms, *J. Geophys. Res.*, *103*, 29419-29428, 1998.

35. Sonnerup, B. U. O., Magnetic field annihilation, in *Solar System Plasma Physics*, vol. 3, ed. by L. J. Lanzerotti, C. F. Kennel, and E. N. Parker, pp. 45-108, North-Holland, New York, 1979.

36. Lui, A. T. Y. and Y. Kamide, A fresh perspective of the substorm current system and its dynamo, *Geophys. Res. Lett.*, *30*, (*18*), 1958, doi:10.1029/2003GL017835, 2003.

37. Lui, A. T. Y., Potential plasma instabilities for substorm expansion onset, *Space Sci. Rev.*, *113*, 127-206, 2004.